



Journal of Modern Optics

Publication details, including instructions for authors and subscription information:

<http://www.tandfonline.com/loi/tmop20>

Analysis of the focal characteristics of cylindrical lenses made of anisotropically dielectric material based on rigorous electromagnetic theory

Bizhen Dong ^a, Jiasheng Ye ^{a b}, Juan Liu ^a, Benyuan Gu ^a, Guozhen Yang ^a, Maohong Lu ^c & Shutian Liu ^a

^a Institute of Physics, Academia Sinica, PO Box 603, Beijing, 100080, China

^b Department of Physics, Harbin Institute of Technology, Harbin, 150001, China

^c Institute of Electro-Optical Engineering, National Chiao Tung University, Hsingchu, Taiwan

Published online: 03 Jul 2009.

To cite this article: Bizhen Dong, Jiasheng Ye, Juan Liu, Benyuan Gu, Guozhen Yang, Maohong Lu & Shutian Liu (2003) Analysis of the focal characteristics of cylindrical lenses made of anisotropically dielectric material based on rigorous electromagnetic theory, Journal of Modern Optics, 50:8, 1195-1208, DOI: [10.1080/09500340308235195](https://doi.org/10.1080/09500340308235195)

To link to this article: <http://dx.doi.org/10.1080/09500340308235195>

PLEASE SCROLL DOWN FOR ARTICLE

Taylor & Francis makes every effort to ensure the accuracy of all the information (the "Content") contained in the publications on our platform. However, Taylor & Francis, our agents, and our licensors make no representations or warranties whatsoever as to the accuracy, completeness, or suitability for any purpose of the Content. Any opinions and views expressed in this publication are the opinions and views of the authors, and are not the views of or endorsed by Taylor & Francis. The accuracy of the Content should not be relied upon and should be independently verified with primary sources of information. Taylor and Francis shall not be liable for any losses, actions, claims, proceedings, demands, costs, expenses, damages,

and other liabilities whatsoever or howsoever caused arising directly or indirectly in connection with, in relation to or arising out of the use of the Content.

This article may be used for research, teaching, and private study purposes. Any substantial or systematic reproduction, redistribution, reselling, loan, sub-licensing, systematic supply, or distribution in any form to anyone is expressly forbidden.

Terms & Conditions of access and use can be found at <http://www.tandfonline.com/page/terms-and-conditions>

Analysis of the focal characteristics of cylindrical lenses made of anisotropically dielectric material based on rigorous electromagnetic theory

BIZHEN DONG^{†*}, JIASHENG YE^{†‡}, JUAN LIU[†],
BENYUAN GU[†], GUOZHEN YANG[†], MAOHONG LU[§] and
SHUTIAN LIU[‡]

[†] Institute of Physics, Academia Sinica, PO Box 603, Beijing 100080, China

[‡] Department of Physics, Harbin Institute of Technology, Harbin, 150001, China

[§] Institute of Electro-Optical Engineering, National Chiao Tung University, Hsingchu, Taiwan

(Received 11 February 2002; revision received 14 June 2002)

Abstract. The focal characteristics of refractive cylindrical lenses made of anisotropically dielectric material (uniaxial crystal) are analysed based on rigorous electromagnetic theory and the boundary element method. The performances of the lenses with different f numbers are appraised for both incident waves of the TE (transverse electric) and TM (transverse magnetic) polarizations. Numerical results show that the focal performance of this kind of lens for the TE polarization and the TM polarization of incident light wave is a difference, in particular, different focal lengths, owing to the anisotropy of the material. However, for the conventional isotropic lens, the focal features for both the TE and TM polarizations are the same. It is anticipated that this new kind of lens proposed for the first time may serve as a light switching device with high speed used in the micro-optical communication.

1. Introduction

Diffraction optical elements have been widely used in various applications to optical interconnections, laser-beam focusing, coupling, feedback, spectral filtering, correlation filtering, wavelength-division multiplexing, signal processing, optical disk readout, beam array generation, and others [1]. The developments of modern microlithography and technologies have made it possible to produce micro-optical elements with small characteristic size comparable to the light wavelength. Because of their small scale, the light-scattering effect in the microlenses becomes more important than that of the light diffraction, thus, the conventional scalar diffraction theory is no longer applicable for analysing the performance of the microlenses. Therefore, the rigorous electromagnetic theory and various numerical methods have been proposed to reveal the features of the microlenses in recent years. One of the effective methods for analysing and

* Author for correspondence; email: bzdong@aphy.iphy.ac.cn

designing microlenses is solving the related integral equations with the use of the boundary element method (BEM) [2–8].

In previous papers the performance of diffractive cylindrical lenses made of isotropically dielectric materials with different f numbers for the TE polarization and the TM polarization has been studied in detail [2, 5, 8]. The results show that the focal characteristics, for instance, the diffractive efficiency and the focal spot size on the focal plane are almost similar with each other for TE and TM polarizations of incident light wave.

In this paper, we study the focal characteristics of the refractive cylindrical lenses made of anisotropic material (uniaxial crystal) with the use of the rigorous electromagnetic theory and BEM. The numerical simulations demonstrate that the focal feature of the TE and TM polarizations of the light wave is a difference, in particular, different focal length owing to the dielectric anisotropy of the material. Diffractive efficiency, focal spot size and focal length of this kind of anisotropic microlens are evaluated for different f number lenses. This paper is organized as follows: in section 2, the basic equations used in the numerical simulations are briefly given. In section 3 the numerical results are presented and a comparison of the focal performance between the isotropically and anisotropically dielectric lenses is also made. Section 4 gives a brief summary. The simple derivation of the relevant formulas used in the calculations is given in Appendix A.

2. Basic equations

A two-dimensional (2D) scattering system in a cylindrical microlens lying on the XY plane is shown in figure 1, in which the boundary Γ with a curved interface divides the 2D space into two semi-infinite regions S_1 and S_2 , and region S_1 is

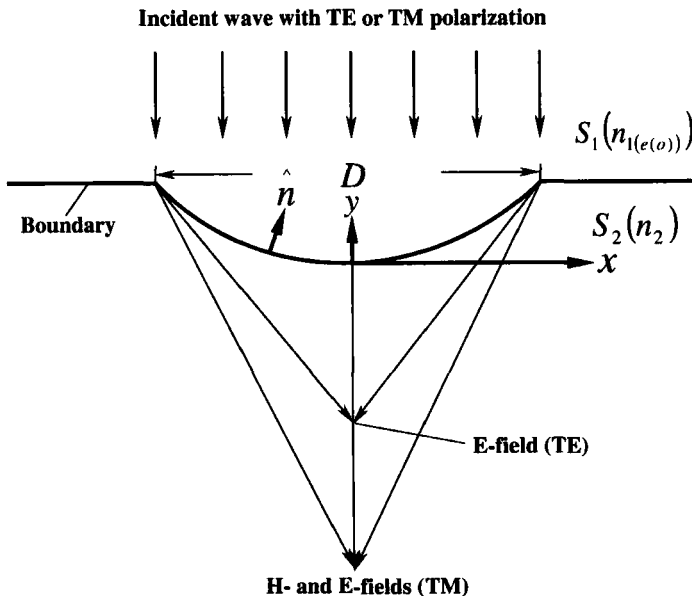


Figure 1. Schematic diagram of a two-dimensional scattering problem in a refractive cylindrical microlens system.

filled by a dielectric material of uniaxial crystal with the optic axis perpendicular to the XY plane, i.e. parallel to the Z axis. The relevant refractive index is $n_{1(e(o))}$ for the TE (TM) polarization of the incident light. Region 2 is filled by an isotropic dielectric material with refractive index of n_2 . The unit vector \hat{n} is normal to the boundary Γ and orients to region S_1 . The incident plane wave is either TE (electric field E_z parallel to the Z axis) or TM (magnetic field H_z parallel to the Z axis) polarization. The amplitude of the incident field is set to 1 in arbitrary units. The plane wave is normally incident upon the boundary Γ on region S_1 and then goes through into region S_2 along the Y axis direction. To determine the transmitted electric field or magnetic field distribution in region S_2 , we apply Green's formula, the radiation condition and Maxwell's equations to derive the integral equations in an isotropic material as follows [2, 5, 6, 9, 10]:

$$-\phi_1(\mathbf{r}_1) + \int_{\Gamma} [\phi_{\Gamma}(\mathbf{r}'_F)\hat{n} \cdot \nabla G_1(\mathbf{r}_1, \mathbf{r}'_F) - p_1 G_1(\mathbf{r}_1, \mathbf{r}'_F)\hat{n} \cdot \nabla \phi_{\Gamma}(\mathbf{r}'_F)] dl' = -\phi^{\text{inc}}(\mathbf{r}_1), \quad (1)$$

$$\phi_2(\mathbf{r}_2) + \int_{\Gamma} [\phi_{\Gamma}(\mathbf{r}'_F)\hat{n} \cdot \nabla G_2(\mathbf{r}_2, \mathbf{r}'_F) - p_2 G_2(\mathbf{r}_2, \mathbf{r}'_F)\hat{n} \cdot \nabla \phi_{\Gamma}(\mathbf{r}'_F)] dl' = 0, \quad (2)$$

where $\phi = E_z$ and $p_i = 1$ for the TE polarization, while $\phi = H_z$ and $p_i = n_i^2$ for the TM polarization. ϕ and ϕ^{inc} stand for the total electric field and the incident electric field, respectively. The subscripts $i = 1$ and 2 represent the quantities in region S_1 and S_2 , respectively. In Appendix A we will give the brief derivation of these equations from Maxwell's equations and boundary conditions, and we will prove that these integral equations are also valid for anisotropically dielectric material (uniaxial crystal) in our particular situation, i.e. the optical axis of the uniaxial crystal is just parallel to the Z axis. The vectors \mathbf{r}_1 , \mathbf{r}_2 , and \mathbf{r}'_F denote the position vectors of points in region S_1 , region S_2 and the boundary Γ , respectively. l' corresponds to the boundary line coordinate at the interface. The boundary conditions on Γ are given by $\phi_1 = \phi_2 = \phi_{\Gamma}$ and $(1/p_1)\hat{n} \cdot \nabla \phi_1 = (1/p_2)\hat{n} \cdot \nabla \phi_2$.

To solve these equations, two unknown quantities, i.e. the fields ϕ_{Γ} and the corresponding normal derivatives $\hat{n} \cdot \nabla \phi_{\Gamma}$ on the boundary, are required to be evaluated first. Let \mathbf{r}_1 and \mathbf{r}_2 approach a point \mathbf{r}_{Γ} on Γ , equations (1) and (2) can then be reduced as follows [2, 5, 6]:

$$\left(\frac{\theta_{\Gamma}}{2\pi} - 1\right)\phi_{\Gamma}(\mathbf{r}_{\Gamma}) + \int_{\Gamma} [\phi_{\Gamma}(\mathbf{r}'_F)\hat{n} \cdot \nabla G_1(\mathbf{r}_{\Gamma}, \mathbf{r}'_F) - p_1 G_1(\mathbf{r}_{\Gamma}, \mathbf{r}'_F)\hat{n} \cdot \nabla \phi_{\Gamma}(\mathbf{r}'_F)] dl' = -\phi^{\text{inc}}(\mathbf{r}_{\Gamma}), \quad (3)$$

$$\left(\frac{\theta_{\Gamma}}{2\pi}\right)\phi_{\Gamma}(\mathbf{r}_{\Gamma}) + \int_{\Gamma} [\phi_{\Gamma}(\mathbf{r}'_F)\hat{n} \cdot \nabla G_2(\mathbf{r}_{\Gamma}, \mathbf{r}'_F) - p_2 G_2(\mathbf{r}_{\Gamma}, \mathbf{r}'_F)\hat{n} \cdot \nabla \phi_{\Gamma}(\mathbf{r}'_F)] dl' = 0, \quad (4)$$

where θ_{Γ} represents the internal angle of Γ at the point \mathbf{r}_{Γ} . The integral specifies Cauchy's principal value of integration. Here Green's function

$$G_i(\mathbf{r}_{\Gamma}, \mathbf{r}'_F) = (-j/4)H_0^{(2)}(k_i|\mathbf{r}_{\Gamma} - \mathbf{r}'_F|) \quad (i = 1, 2) \quad (5)$$

is adopted. $H_0^{(2)}$ is the zero-order Hankel function of the second kind and $k_i = n_i k_0$ ($i = 1, 2$), where k_0 is the wave number of light in free space and $k_0 = 2\pi/\lambda_0$, where λ_0 is the wavelength of the incident light in free space.

Table 1. The relevant parameters used in equations for both isotropically and anisotropically dielectric lenses.^a

Dielectric materials	Polarization	Field	$k_i = n_i k_0$	p_i
Isotropic	TE	E_z	$k_1 = n_1 k_0$ $k_2 = n_2 k_0$	$p_1 = 1$ $p_2 = 1$
	TM	H_z	$k_1 = n_1 k_0$ $k_2 = n_2 k_0$	$p_1 = n_1^2$ $p_2 = n_2^2$
Anisotropic	TE	E_z	$k_1 = n_{1(e)} k_0$ $k_2 = n_2 k_0$	$p_1 = 1$ $p_2 = 1$
	TM	H_z	$k_1 = n_{1(o)} k_0$ $k_2 = n_2 k_0$	$p_1 = n_{1(o)}^2$ $p_2 = n_2^2$

^a Note that $n_{1(o)}$ and $n_{1(e)}$ represent the refractive indices for the ordinary and extraordinary light wave in uniaxial crystal, respectively.

By employing the BEM [2, 5, 6, 10–12] to solve equations (1)–(4), the electric field E and their normal derivatives $\hat{n} \cdot \nabla E$ on the boundary with $p_i = 1$ for the TE polarization as well as the magnetic field H and their derivatives $\hat{n} \cdot \nabla H$ on the boundary with $p_i = n_i^2$ for the TM polarization can be obtained. To explicitly demonstrate the difference of the parameters appearing in the equations (1)–(4) for isotropically and anisotropically dielectric lenses, we prefer to tabulate them in table 1.

We usually measure only the \mathbf{E} field distribution rather than the \mathbf{H} field distribution, therefore, we need to convert the \mathbf{H} field into \mathbf{E} field for the TM polarization. According to the electromagnetic theory, the waves relationship between the \mathbf{E} and \mathbf{H} fields (see Appendix A for details) is given by

$$\begin{aligned}
 \mathbf{E} &= \frac{i}{\omega \epsilon_0} \epsilon^{-1} (\nabla \times \mathbf{H}) \\
 &= \frac{i}{\omega \epsilon_0} \begin{pmatrix} \frac{1}{\epsilon_a} & 0 & 0 \\ 0 & \frac{1}{\epsilon_b} & 0 \\ 0 & 0 & \frac{1}{\epsilon_c} \end{pmatrix} \begin{pmatrix} \frac{\partial H_z}{\partial y} \\ -\frac{\partial H_z}{\partial x} \\ 0 \end{pmatrix} \\
 &= \frac{i}{\omega \epsilon_0} \begin{pmatrix} \frac{1}{\epsilon_a} \frac{\partial H_z}{\partial y} \\ -\frac{1}{\epsilon_b} \frac{\partial H_z}{\partial x} \\ 0 \end{pmatrix}, \tag{6}
 \end{aligned}$$

where ω and ϵ_0 denote the circular frequency of the light wave and the permittivity in vacuum, respectively. For isotropic material we have $\epsilon_a = \epsilon_b = \epsilon$ for any polarization, however, in a uniaxial crystal we have $\epsilon_a = \epsilon_b = \epsilon_o$ with $\epsilon_o = n_o^2$ for the TM polarization alone. Finally, the total electric field for TM polarization can be synthesized as

$$E(x, y) = (|E_x|^2 + |E_y|^2)^{1/2}. \tag{7}$$

To evaluate the focusing action of the microlens, we define the diffraction efficiency η as

$$\eta = \frac{\int_{-d/2}^{d/2} I_f(x_2, y_2) dx_2}{\int_{-R}^R I_{inc}(x_1, y_1) dx_1}, \tag{8}$$

where d denotes the focal spot size, which is defined as the minimum-to-minimum width of the main lobe of the intensity profile on the focal plane; $2R$ denotes the size of the aperture of the incident light wave. $I_{inc}(x_1, y_1)$ and $I_f(x_2, y_2)$ indicate the incident light wave intensity at the aperture and the focused beam intensity on the focal plane, respectively.

3. Numerical simulations

3.1. For isotropic microlenses

We first consider 2D space filled with two isotropically dielectric materials, such as glass in region S_1 and air in region S_2 . A plane wave with wavelength $\lambda = 0.488 \mu\text{m}$ in free space is normally incident from region S_1 upon the curved interface of the microlens, as shown in figure 1. Assume that the chosen parameters of the refractive cylindrical lens are: the size of the aperture of the lens is $D = 30 \mu\text{m}$; the nominal focal lengths of the lenses are selected as 120, 60, and $45 \mu\text{m}$, i.e. the f number of the lenses is $f/4$, $f/2$ and $f/1.5$. The refractive indices n_1 and n_2 are chosen as $n_1 = 1.5$ for glass and $n_2 = 1.0$ for air.

To reveal the performance of the microlens for the TE and TM polarizations, the intensity profile on the focal plane usually provides an important indication for the focusing function. We calculate the intensity distributions of the \mathbf{E} field for the TE polarization, and the \mathbf{H} and \mathbf{E} fields for the TM polarization on both the axial and lateral directions according to equations (1)–(4) and (7) with the use of the BEM. The numerical results, including the focal spot size, the focal length and the diffraction efficiency, are summarized in table 2 for the $f/4$, $f/2$ and $f/1.5$ lenses. From the results of table 2, it is clearly seen that the focal spot sizes of the \mathbf{E} and \mathbf{H} fields for the TE and TM polarizations are very close to each other for each individual f number. The focal spot size and the focal length in the \mathbf{E} (\mathbf{H}) field of

Table 2. Focal spot size, focal length, diffraction efficiency of \mathbf{E} and \mathbf{H} fields (for the TE or TM polarizations) of microlenses made of isotropically dielectric material (region S_1) with different f numbers.

Lens	Focal spot size (μm)			Focal spot size (μm)			Diffraction efficiency (%)		
	TE	TM		TE	TM		TE	TM	
$f/\#$	\mathbf{E} field	\mathbf{H} field	\mathbf{E} field	\mathbf{E} field	\mathbf{H} field	\mathbf{E} field	\mathbf{E} field	\mathbf{H} field	\mathbf{E} field
$f/4$	3.72	3.72	3.74	116.34	116.34	116.16	89.41	89.31	89.25
$f/2$	1.94	1.92	1.96	56.81	56.81	56.81	85.48	84.94	84.62
$f/1.5$	1.47	1.44	1.49	40.91	40.82	40.91	79.84	78.41	77.86

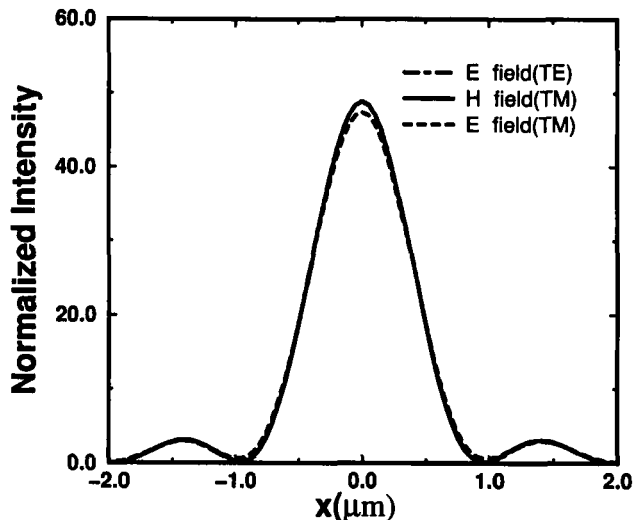


Figure 2. Lateral intensity distribution on the focal plane for the $f/2$ lens with an isotropically dielectric material.

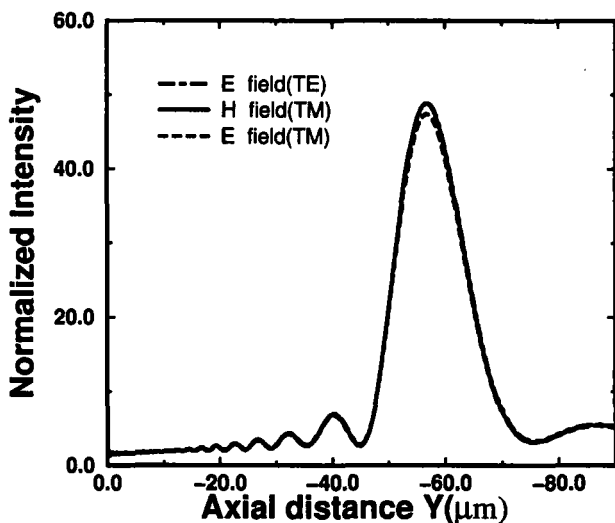


Figure 3. Axial intensity distribution for the $f/2$ lens with an isotropically dielectric material.

the TM polarization and the \mathbf{E} field of the TE polarization are almost the same for each individual $f/\#$. Their diffractive efficiencies only exhibit a small difference. In order to present a good view, we display the lateral intensity distributions on the focal planes in figure 2 for the \mathbf{E} field (TE) (dot-dashed curve), the \mathbf{H} field (TM) (solid curve) and \mathbf{E} field (TM) (dashed curve) distributions in the case of the $f/2$ lens. It is evident that the spot sizes are very close to each other.

The axial focusing situation of the \mathbf{E} field (TE), the \mathbf{H} field (TM) and the \mathbf{E} field (TM) remains similar for each f number. Figure 3 displays the axial intensity

distributions of the **E** field (TE) (dot-dashed curve), the **H** field (TM) (solid curve) and the **E** field (TM) (dashed curve) for the $f/2$ lens in region S_2 . It is clearly seen from figure 3 that the peaks of the focal intensity for the three fields are almost located at the same plane.

3.2. For anisotropic microlenses

We now investigate the performance of the microlens when the isotropic material is replaced by anisotropic material (uniaxial crystal) in region S_1 , as shown in figure 1. The incident light beam normally impinges onto the surface of the lens. The optic axis is taken along the Z axis. In particular, we consider the uniaxial crystal of titanium dioxide (TiO_2) with the extraordinary light index, $n_{1(e)} = 3.06$, for the TE polarization and the ordinary light index, $n_{1(o)} = 2.73$, for the TM polarization when the wavelength of the incident beam is chosen as $0.488\ \mu\text{m}$ [13]. The other parameters used are the same as those in the above isotropic microlens system. The numerical simulations are summarized in table 3. It is seen from table 3 that the focal spot size of the focal **E** (**H**) field for the TM polarization is quite a bit larger than that of the **E** field (TE) for all the f numbers considered. The spot size of the **E** field (TM) is a little larger than that of the corresponding **H** field (TM) for each individual lens.

The focal lengths of the **H** and **E** fields of the TM polarization listed in table 3 are identical with each other, however, they are much longer than the focal length of the **E** field (TE) for every corresponding f number lens. This means that the focal **E** fields for the TE and TM polarizations remarkably shift away from each other along the direction of the light beam propagation. The shift distance is decreased with decreasing f number of the lens. For instance, the shift distances are 20.71 , 11.44 and $8.90\ \mu\text{m}$ for the $f/4$, $f/2$ and $f/1.5$ lenses, respectively. However, when accounting for the relative shift quantity of $[f_{TM} - f_{TE}]/[0.5(f_{TM} + f_{TE})]$, we find that this quantity is increased with $f/\#$; for instance, their corresponding values are 0.1616 , 0.1758 and 0.1854 for the above-mentioned $f/\#$. The diffractive efficiency of the **H** (TM) and **E** fields (TE, TM) is also shown in table 3, the values are also close to each other for each individual f number lens. The diffractive efficiency is decreased with decreasing $f/\#$.

We now display the lateral intensity distributions of the **E** field (TE) and the **E** (**H**) field (TM) of an anisotropically dielectric lens at the focal plane, fixed $f/2$, in figure 4. The dot-dashed curve corresponds to the **E** field (TE), the solid curve to the **H** field (TM) and the dashed curve to the **E** field (TM). It is evident that the

Table 3. Same as table 2 except that in region S_1 filled with anisotropically dielectric material (uniaxial crystal).

Lens	Focal spot size (μm)			Focal spot size (μm)			Diffraction efficiency (%)		
	TE	TM		TE	TM		TE	TM	
$f/\#$	E field	H field	E field	E field	H field	E field	E field	H field	E field
$f/4$	3.75	4.39	4.41	117.79	138.50	138.50	89.74	89.78	89.78
$f/2$	1.98	2.31	2.35	59.35	70.79	70.79	87.07	87.54	87.37
$f/1.5$	1.51	1.77	1.82	44.00	52.90	52.90	85.23	85.61	85.33

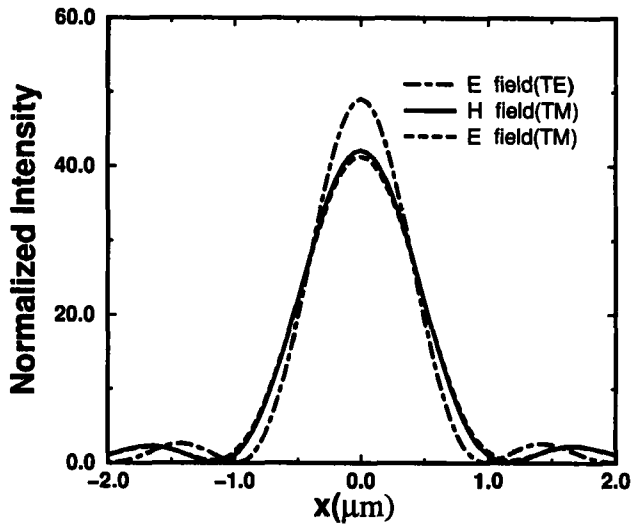


Figure 4. Same as figure 2, but the isotropically dielectric material is replaced by an anisotropically dielectric material.

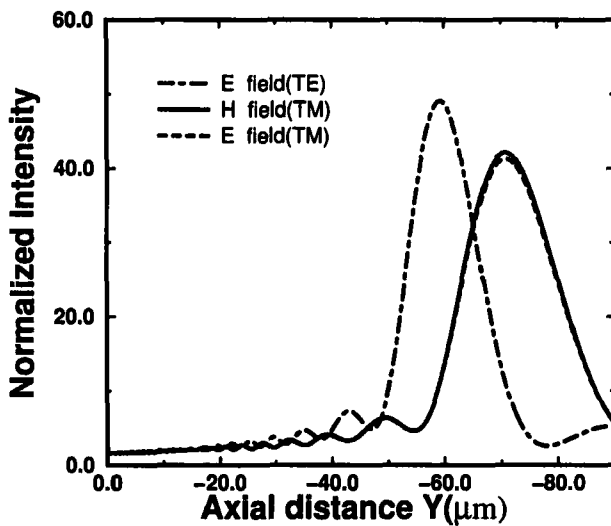


Figure 5. Same as figure 3, but the isotropically dielectric material is replaced by an anisotropically dielectric material.

focal spot size of the \mathbf{E} field (TE) is quite a bit smaller than that of the \mathbf{E} (\mathbf{H}) field (TM). We plot the axial intensity distribution (around the focal region) of the relevant fields to show the shift of the position of the focal plane in figure 5, fixed $f/2$. The dot-dashed curve corresponds to the \mathbf{E} field (TE), the solid curve to the \mathbf{H} field (TM), and the dashed curve to the \mathbf{E} field (TM). It is apparent that the location of the focal plane for the TE polarization is closer to the surface of the lens than that for the TM polarization owing to $n_{1(e)} = 3.06$ and $n_{1(o)} = 2.73$ in our particular case. We can evaluate this shift of the focal position through a simple

argument as follows: according to the simple relationship between the focal length f and material refractive index n of $f = r/(n - 1)$, for a cylindrical lens in figure 1, the TE and TM polarized waves focus at $f_{TE} = r/(n_e - 1)$, $f_{TM} = r/(n_o - 1)$, respectively, where r denotes the curvature of the lens with a single curving surface. This indicates that $f_{TM}/f_{TE} = (n_e - 1)/(n_o - 1) = 1.19$, which agrees well with the results given in table 3, for instance, $f_{TM}/f_{TE} = 1.176, 1.193$ and 1.202 for $f/\# = f/4, f/2$ and $f/1.5$, respectively.

4. Summary

The focusing characteristics of both isotropically and anisotropically refractive cylindrical lenses with different f numbers have been analysed with the use of the rigorous electromagnetic theory and boundary element method. The expressions of conversion from the \mathbf{H} field into the \mathbf{E} field for the TM polarization are given. The lateral and axial intensity distributions of the \mathbf{E} (\mathbf{H}) field for the TM polarization and \mathbf{E} field for the TE polarization are calculated. The focusing performance of the lens, including the focal spot size, the focal length and the diffraction efficiency are appraised. We also compare the features between the isotropically and anisotropically dielectric material lenses for the case of a normally incident light wave. The numerical simulations show that in the case of isotropic dielectricity the \mathbf{E} and \mathbf{H} field distributions for the TE and TM polarizations exhibit almost the same focusing behaviour for different f numbers. However, in the case of anisotropic dielectricity, we found that the focal spot size of the \mathbf{E} field (TM) is quite a bit larger than that of the \mathbf{E} field (TE). It is noted that the positions of the focal plane of the \mathbf{E} field for the TE and TM polarizations shift remarkably away from each other. The focal length of the \mathbf{E} field (TE) is shorter than that of the \mathbf{E} field (TM). This result can be understood from the simple argument owing to the difference of the refraction index of the uniaxial crystal for two polarizations. These interesting features are reported here for the first time. It is expected that these kinds of elements might serve as ideal light switching devices with high speed in micro-optical communication.

Acknowledgments

This work was supported by the Major State Basic Research Development Program 'Integrated Micro-Optical-Electro-Mechanical Systems' under contact G1999033104 in China.

Appendix A: Derivation of the boundary integral equations for anisotropically dielectric lens

In this appendix we present the boundary integral equations appropriate for anisotropic material. In anisotropic medium, material equations can be written as

$$\begin{aligned}\mathbf{D} &= \varepsilon_0 \boldsymbol{\varepsilon} \mathbf{E}, \\ \mathbf{B} &= \mu_0 \boldsymbol{\mu} \mathbf{H},\end{aligned}\tag{A 1}$$

where ε_0 and $\boldsymbol{\varepsilon}$ represent the permittivity in vacuum and the dielectric tensor of the material, respectively. μ_0 and $\boldsymbol{\mu}$ represent the magnetic permeability in vacuum

and the medium, respectively. For a harmonic field with angular frequency ω , from Maxwell's equations, we can derive the wave equation for an anisotropic material

$$\nabla \times [\nabla \times \mathbf{E}(\mathbf{r})] = \frac{\omega^2}{c^2} \boldsymbol{\varepsilon}(\mathbf{r}) \boldsymbol{\mu}(\mathbf{r}) \mathbf{E}(\mathbf{r}). \quad (\text{A } 2)$$

In the system of principal dielectric axes, the dielectric tensor is diagonalized as [14]:

$$\boldsymbol{\varepsilon} = \begin{pmatrix} \varepsilon_a & 0 & 0 \\ 0 & \varepsilon_b & 0 \\ 0 & 0 & \varepsilon_c \end{pmatrix} \quad (\text{A } 3)$$

Especially for a uniaxial crystal $\varepsilon_a = \varepsilon_b = \varepsilon_o$, $\varepsilon_c = \varepsilon_e$, where ε_o and ε_e represent the permittivity of the ordinary wave and the extraordinary wave, respectively.

In the two-dimensional cylindrical boundary case as shown in figure 1, for the TE polarization, the electric field $\mathbf{E} = E_z \mathbf{e}_3$, $E_x = E_y = 0$ and $\partial/\partial z = 0$. Equation (A 2) is reduced to

$$\nabla^2 \mathbf{E} + k^2 \mathbf{E} = 0,$$

where $k = (\omega/c)\varepsilon_e^{1/2} = \omega n_e/c$.

We now introduce Green's function $G_i(\mathbf{r}, \mathbf{r}') = (1/4j)H_0(k_i|\mathbf{r} - \mathbf{r}'|)$, which satisfies

$$\nabla^2 G_i(\mathbf{r}, \mathbf{r}') + k^2 G_i(\mathbf{r}, \mathbf{r}') = -\delta(\mathbf{r} - \mathbf{r}'). \quad (\text{A } 4)$$

By applying the well-known Green's theorem, we obtain

$$\begin{aligned} \iint_{\Omega_2} G_2(\mathbf{r}, \mathbf{r}') \nabla^2 \mathbf{E}_2(\mathbf{r}') d\Omega &= \iint_{\Omega_2} \mathbf{E}_2(\mathbf{r}') \nabla^2 G_2(\mathbf{r}, \mathbf{r}') d\Omega \\ &+ \int_{\Gamma_2} \left[G_2(\mathbf{r}, \mathbf{r}') \frac{\partial \mathbf{E}_2(\mathbf{r}')}{\partial \mathbf{n}_2} - \mathbf{E}_2(\mathbf{r}') \frac{\partial G_2(\mathbf{r}, \mathbf{r}')}{\partial \mathbf{n}_2} \right] dl', \end{aligned} \quad \mathbf{r} \in S_2, \quad (\text{A } 5)$$

where \mathbf{n}_2 is the outward unit vector of the boundary of region S_2 . All the quantities labelled by 2 belong to region S_2 . From figure 1, we have $\mathbf{n} = \mathbf{n}_2 = -\mathbf{n}_1$.

Substituting (A 4) and the wave equation into (A 5), we obtain

$$\mathbf{E}_2(\mathbf{r}) + \int_{\Gamma_2} \left[\mathbf{E}_2(\mathbf{r}') \frac{\partial G_2(\mathbf{r}, \mathbf{r}')}{\partial \mathbf{n}} - G_2(\mathbf{r}, \mathbf{r}') \frac{\partial \mathbf{E}_2(\mathbf{r}')}{\partial \mathbf{n}} \right] dl' = 0, \quad \mathbf{r} \in S_2. \quad (\text{A } 6)$$

When $\mathbf{r} \rightarrow \mathbf{r}_\Gamma$, singularities occur in the above integral [12] and we evaluate

$$\begin{aligned} \lim_{\rho \rightarrow 0} \int \mathbf{E} \frac{\partial G}{\partial \mathbf{n}} d\Gamma &= \lim_{\rho \rightarrow 0} \left\{ \rho(2\pi - \theta_\Gamma) \left[-\frac{k}{4j} H_1^{(2)}(k\rho) \right] \mathbf{E} \right\} \\ &= j \frac{k(2\pi - \theta_\Gamma)}{4} \lim_{\rho \rightarrow 0} \left\{ \rho \left[\frac{k\rho}{2} - j \left(-\frac{1}{\pi} \right) \frac{2}{k\rho} \right] \mathbf{E} \right\} \\ &= \left(\frac{\theta_\Gamma}{2\pi} - 1 \right) \mathbf{E}; \end{aligned} \quad (\text{A } 7)$$

$$\begin{aligned} \lim_{\rho \rightarrow 0} \int G \frac{\partial \mathbf{E}}{\partial \mathbf{n}} d\Gamma &= \lim_{\rho \rightarrow 0} \left\{ \rho(2\pi - \theta_\Gamma) \left[\frac{1}{4j} H_0^{(2)}(k\rho) \right] \frac{\partial \mathbf{E}}{\partial \mathbf{n}} \right\} \\ &= -j \frac{2\pi - \theta_\Gamma}{4} \lim_{\rho \rightarrow 0} \left\{ \rho \left[1 - j \frac{2}{\pi} \left(\ln \frac{k\rho}{2} + \gamma \right) \right] \frac{\partial \mathbf{E}}{\partial \mathbf{n}} \right\} = 0, \end{aligned} \quad (\text{A } 8)$$

where θ_Γ is the internal angle of the boundary and γ is the Euler number with $\gamma = 0.577\ 215$.

Equation (A 8) is then simplified as

$$\left(\frac{\theta_\Gamma}{2\pi} \right) \mathbf{E}_2(\mathbf{r}_\Gamma) + \int_\Gamma \left[\mathbf{E}_2(\mathbf{r}'_\Gamma) \frac{\partial G_2(\mathbf{r}_\Gamma, \mathbf{r}'_\Gamma)}{\partial \mathbf{n}} - G_2(\mathbf{r}_\Gamma, \mathbf{r}'_\Gamma) \frac{\partial \mathbf{E}_2(\mathbf{r}'_\Gamma)}{\partial \mathbf{n}} \right] dl' = 0, \quad (\text{A } 9)$$

where \int_Γ represents Cauchy's principal value of integration.

In region S_1 , where the incident wave is originated, the wave equation should be written as $\nabla^2 \mathbf{E}(\mathbf{r}) + k^2 \mathbf{E}(\mathbf{r}) = -f(\mathbf{r})$. Here $f(\mathbf{r})$ is the light source term with $\phi^{\text{inc}}(\mathbf{r}) = \int f(\mathbf{r}') G_1(\mathbf{r}, \mathbf{r}') dl'$, which is the incident field. Following the above steps, the boundary integral equation of S_1 can be derived

$$\left(\frac{\theta_\Gamma}{2\pi} - 1 \right) \mathbf{E}_1(\mathbf{r}_\Gamma) + \int_\Gamma \left[\mathbf{E}_1(\mathbf{r}'_\Gamma) \frac{\partial G_1(\mathbf{r}_\Gamma, \mathbf{r}'_\Gamma)}{\partial \mathbf{n}} - G_1(\mathbf{r}_\Gamma, \mathbf{r}'_\Gamma) \frac{\partial \mathbf{E}_1(\mathbf{r}'_\Gamma)}{\partial \mathbf{n}} \right] dl' = -\phi^{\text{inc}}(\mathbf{r}_\Gamma). \quad (\text{A } 10)$$

For the TM polarization, we first give the wave equation in an anisotropic material. According to Maxwell's equation, $\nabla \times \mathbf{H} = (\partial \mathbf{D} / \partial t) = -i\omega \epsilon_0 \epsilon \mathbf{E}$, therefore, we have

$$\nabla \times (\nabla \times \mathbf{H}) = -i\omega \epsilon_0 [\nabla \times (\epsilon \mathbf{E})]. \quad (\text{A } 11)$$

From equation (A 3) and Maxwell's equation, we have $E_z = 0$. The right side of equation (A 11) is

$$\nabla \times (\epsilon \mathbf{E}) = \nabla \times \left[\begin{pmatrix} \epsilon_a & 0 & 0 \\ 0 & \epsilon_b & 0 \\ 0 & 0 & \epsilon_c \end{pmatrix} \begin{pmatrix} E_x \\ E_y \\ 0 \end{pmatrix} \right] = \begin{pmatrix} -\epsilon_b \frac{\partial E_y}{\partial z} \\ \epsilon_a \frac{\partial E_x}{\partial z} \\ \epsilon_b \frac{\partial E_y}{\partial x} - \epsilon_a \frac{\partial E_x}{\partial y} \end{pmatrix}.$$

In the case of the TM polarization, the magnetic field $\mathbf{H} = H_z \mathbf{e}_3$, $H_x = H_y = 0$ and $(\partial / \partial z) = 0$. As $\nabla \cdot \mathbf{H} = 0$, therefore, $\nabla \times (\nabla \times \mathbf{H}) = -\nabla^2 \mathbf{H}$ is valid, thus, wave equation (A 11) can be written as

$$-\nabla^2 \mathbf{H} + i\omega \epsilon_0 \left(\epsilon_b \frac{\partial E_y}{\partial x} - \epsilon_a \frac{\partial E_x}{\partial y} \right) = 0. \quad (\text{A } 12)$$

For a uniaxial crystal, $\epsilon_a = \epsilon_b = \epsilon_0$, and considering Maxwell's equation $\nabla \times \mathbf{E} = i\omega \mu \mathbf{H}$, we obtain

$$\nabla^2 \mathbf{H} + k^2 \mathbf{H} = 0,$$

where $k = (\omega/c) \epsilon_0^{1/2} = (\omega n_0/c)$.

The corresponding boundary integral equations for the TM polarization are

$$\begin{aligned} \left(\frac{\theta_\Gamma}{2\pi} - 1\right) \mathbf{H}_1(\mathbf{r}_\Gamma) + \int_\Gamma \left[\mathbf{H}_1(\mathbf{r}'_\Gamma) \frac{\partial G_1(\mathbf{r}_\Gamma, \mathbf{r}'_\Gamma)}{\partial \mathbf{n}} - G_1(\mathbf{r}_\Gamma, \mathbf{r}'_\Gamma) \frac{\partial \mathbf{H}_1(\mathbf{r}'_\Gamma)}{\partial \mathbf{n}} \right] dl' &= -\phi^{\text{inc}}(\mathbf{r}_\Gamma), \\ \left(\frac{\theta_\Gamma}{2\pi}\right) \mathbf{H}_2(\mathbf{r}_\Gamma) + \int_\Gamma \left[\mathbf{H}_2(\mathbf{r}'_\Gamma) \frac{\partial G_2(\mathbf{r}_\Gamma, \mathbf{r}'_\Gamma)}{\partial \mathbf{n}} - G_2(\mathbf{r}_\Gamma, \mathbf{r}'_\Gamma) \frac{\partial \mathbf{H}_2(\mathbf{r}'_\Gamma)}{\partial \mathbf{n}} \right] dl' &= 0. \end{aligned} \quad (\text{A } 13)$$

After we calculate the \mathbf{H} field distribution, we can easily compute the corresponding \mathbf{E} field distribution. From equations (A 3) and $\nabla \times \mathbf{H} = -i\omega\epsilon_0\epsilon\mathbf{E}$, we can calculate that

$$\mathbf{E} = \frac{i}{\omega\epsilon_0} \boldsymbol{\epsilon}^{-1} (\nabla \times \mathbf{H}) = \frac{i}{\omega\epsilon_0} \begin{pmatrix} \frac{1}{\epsilon_a} & 0 & 0 \\ 0 & \frac{1}{\epsilon_b} & 0 \\ 0 & 0 & \frac{1}{\epsilon_c} \end{pmatrix} \begin{pmatrix} \frac{\partial H_z}{\partial y} \\ -\frac{\partial H_z}{\partial x} \\ 0 \end{pmatrix} = \frac{i}{\omega\epsilon_0} \begin{pmatrix} \frac{1}{\epsilon_a} \frac{\partial H_z}{\partial y} \\ -\frac{1}{\epsilon_b} \frac{\partial H_z}{\partial x} \\ 0 \end{pmatrix}. \quad (\text{A } 14)$$

We now turn to discuss the boundary conditions for the TE and TM polarizations in a uniaxial crystal, used for the ultimate boundary integral equations. For two dielectric media, the boundary conditions of the field across the interface are

$$\left. \begin{aligned} \mathbf{n} \times (\mathbf{E}_1 - \mathbf{E}_2) &= 0 \\ \mathbf{n} \cdot (\mathbf{D}_1 - \mathbf{D}_2) &= 0 \end{aligned} \right\} \text{ for the electric field,}$$

and

$$\left. \begin{aligned} \mathbf{n} \times (\mathbf{H}_1 - \mathbf{H}_2) &= 0 \\ \mathbf{n} \cdot (\mathbf{B}_1 - \mathbf{B}_2) &= 0 \end{aligned} \right\} \text{ for the magnetic field.}$$

Only two of the above four equations are independent. Now we select $\mathbf{n} \times (\mathbf{E}_1 - \mathbf{E}_2) = 0$, and $\mathbf{n} \times (\mathbf{H}_1 - \mathbf{H}_2) = 0$. First, we consider the case of the TE polarization, i.e. $\mathbf{E} = E_x \mathbf{e}_3$, thus $\mathbf{n} \times (\mathbf{E}_1 - \mathbf{E}_2) = 0$; we get

$$\mathbf{E}_1 = \mathbf{E}_2 = \phi_\Gamma. \quad (\text{A } 15)$$

On the other hand, we have

$$\begin{aligned} \mathbf{n} \times \mathbf{H} &= \mathbf{n} \times \left[-\frac{i}{\omega\mu} (\nabla \times \mathbf{E}) \right] = -\frac{i}{\omega\mu} [\mathbf{n} \times (\nabla \times \mathbf{E})] \\ &= -\frac{i}{\omega\mu} [-\mathbf{n} \cdot \nabla \mathbf{E} + \nabla(\mathbf{n} \cdot \mathbf{E})]. \end{aligned} \quad (\text{A } 16)$$

With $\mathbf{n} \cdot \mathbf{E} = 0$, equation (A 16) can be reduced to $\mathbf{n} \times \mathbf{H} = (i/\omega\mu)(\mathbf{n} \cdot \nabla \mathbf{E}) = (i/\omega\mu)(\partial \mathbf{E} / \partial \mathbf{n})$.

Therefore, we obtain

$$\mathbf{n} \times (\mathbf{H}_1 - \mathbf{H}_2) = i \left[\frac{1}{\omega\mu_1} \frac{\partial \mathbf{E}_1}{\partial \mathbf{n}} - \left(\frac{1}{\omega\mu_2} \frac{\partial \mathbf{E}_2}{\partial \mathbf{n}} \right) \right].$$

As $\mu_1 = \mu_2 = 1$, then we have

$$\frac{\partial \mathbf{E}_1}{\partial \mathbf{n}} = \frac{\partial \mathbf{E}_2}{\partial \mathbf{n}} = \psi_\Gamma. \tag{A 17}$$

Applying boundary conditions (A 15) and (A 17) to the boundary integral equations (A 9) and (A 10), we obtain the final boundary integral equations for the TE polarization as

$$\begin{aligned} \left(\frac{\theta_\Gamma}{2\pi} - 1\right) \phi_\Gamma(\mathbf{r}_\Gamma) + \int_\Gamma \left[\phi_\Gamma(\mathbf{r}'_\Gamma) \frac{\partial G_1(\mathbf{r}_\Gamma, \mathbf{r}'_\Gamma)}{\partial \mathbf{n}} - G_1(\mathbf{r}_\Gamma, \mathbf{r}'_\Gamma) \frac{\partial \phi_\Gamma(\mathbf{r}'_\Gamma)}{\partial \mathbf{n}} \right] dl' &= -\phi^{\text{inc}}(\mathbf{r}_\Gamma), \\ \left(\frac{\theta_\Gamma}{2\pi}\right) \phi_\Gamma(\mathbf{r}_\Gamma) + \int_\Gamma \left[\phi_\Gamma(\mathbf{r}'_\Gamma) \frac{\partial G_2(\mathbf{r}_\Gamma, \mathbf{r}'_\Gamma)}{\partial \mathbf{n}} - G_2(\mathbf{r}_\Gamma, \mathbf{r}'_\Gamma) \frac{\partial \phi_\Gamma(\mathbf{r}'_\Gamma)}{\partial \mathbf{n}} \right] dl' &= 0. \end{aligned} \tag{A 18}$$

We now consider the TM polarization, that is, $\mathbf{H} = H_z \mathbf{e}_3$, $H_x = H_y = 0$, $E_z = 0$. As \mathbf{n} is perpendicular to \mathbf{H} in this case, we then have

$$\mathbf{H}_1 = \mathbf{H}_2 = \phi_\Gamma. \tag{A 19}$$

Meanwhile, by using equation (A 14), we have

$$\mathbf{n} \times \mathbf{E} = \mathbf{n} \times \frac{i}{\omega \varepsilon_0} \begin{pmatrix} \frac{1}{\varepsilon_a} \frac{\partial H_z}{\partial y} \\ -\frac{1}{\varepsilon_b} \frac{\partial H_z}{\partial x} \\ 0 \end{pmatrix} = -\frac{i}{\omega \varepsilon_0} \left(n_x \frac{1}{\varepsilon_b} \frac{\partial H_z}{\partial x} + n_y \frac{1}{\varepsilon_a} \frac{\partial H_z}{\partial y} \right) \mathbf{e}_3, \tag{A 20}$$

where $\mathbf{n} = n_x \mathbf{i} + n_y \mathbf{j}$, which is the outward unit normal vector of the boundary. We now define $n'_x = n_x(1/\varepsilon_b)$, $n'_y = n_y(1/\varepsilon_a)$, and $\mathbf{n}' = n'_x \mathbf{i} + n'_y \mathbf{j}$. Because $\mathbf{n} \times (\mathbf{E}_1 - \mathbf{E}_2) = 0$, we then get

$$\mathbf{n} \times (\mathbf{E}_1 - \mathbf{E}_2) = -\frac{i}{\omega \varepsilon_0} \frac{\partial \mathbf{H}_1}{\partial \mathbf{n}'_1} + \frac{i}{\omega \varepsilon_0} \frac{\partial \mathbf{H}_2}{\partial \mathbf{n}'_2} = 0.$$

It means that

$$\frac{\partial \mathbf{H}_1}{\partial \mathbf{n}'_1} = \frac{\partial \mathbf{H}_2}{\partial \mathbf{n}'_2} = \psi_\Gamma. \tag{A 21}$$

As $\varepsilon_a = \varepsilon_b = \varepsilon_o$ in the uniaxial crystal, therefore, $\varepsilon_1 \mathbf{n}'_1 = \varepsilon_2 \mathbf{n}'_2 = \mathbf{n}$. Finally, we can get the boundary integral equations for the TM polarization as

$$\begin{aligned} \left(\frac{\theta_\Gamma}{2\pi} - 1\right) \phi_\Gamma(\mathbf{r}_\Gamma) + \int_\Gamma \left[\phi_\Gamma(\mathbf{r}'_\Gamma) \frac{\partial G_1(\mathbf{r}_\Gamma, \mathbf{r}'_\Gamma)}{\partial \mathbf{n}} - \varepsilon_1 G_1(\mathbf{r}_\Gamma, \mathbf{r}'_\Gamma) \frac{\partial \phi_\Gamma(\mathbf{r}'_\Gamma)}{\partial \mathbf{n}} \right] dl' &= -\phi^{\text{inc}}(\mathbf{r}_\Gamma), \\ \left(\frac{\theta_\Gamma}{2\pi}\right) \phi_\Gamma(\mathbf{r}_\Gamma) + \int_\Gamma \left[\phi_\Gamma(\mathbf{r}'_\Gamma) \frac{\partial G_2(\mathbf{r}_\Gamma, \mathbf{r}'_\Gamma)}{\partial \mathbf{n}} - \varepsilon_2 G_2(\mathbf{r}_\Gamma, \mathbf{r}'_\Gamma) \frac{\partial \phi_\Gamma(\mathbf{r}'_\Gamma)}{\partial \mathbf{n}} \right] dl' &= 0. \end{aligned} \tag{A 22}$$

It should be mentioned that in equation (A 22), $\varepsilon_1 = \varepsilon_o = n_o^2$ and n_o is the index of ordinary light in the uniaxial crystal.

To sum up, the boundary integral equations are expressed as

$$\left(\frac{\theta_r}{2\pi} - 1\right)\phi_r(\mathbf{r}_r) + \int_r \left[\phi_r(\mathbf{r}'_r) \frac{\partial G_1(\mathbf{r}_r, \mathbf{r}'_r)}{\partial \mathbf{n}} - p_1 G_1(\mathbf{r}_r, \mathbf{r}'_r) \frac{\partial \phi_r(\mathbf{r}'_r)}{\partial \mathbf{n}} \right] dl' = -\phi^{\text{inc}}(\mathbf{r}_r),$$

$$\left(\frac{\theta_r}{2\pi}\right)\phi_r(\mathbf{r}_r) + \int_r \left[\phi_r(\mathbf{r}'_r) \frac{\partial G_2(\mathbf{r}_r, \mathbf{r}'_r)}{\partial \mathbf{n}} - p_2 G_2(\mathbf{r}_r, \mathbf{r}'_r) \frac{\partial \phi_r(\mathbf{r}'_r)}{\partial \mathbf{n}} \right] dl' = 0, \quad (\text{A } 23)$$

where $p_i = 1$ and $\phi = E_z$ for the TE polarization; while $p_i = n_i^2$ and $\phi = H_z$ for the TM polarization. We should note that in the uniaxial crystal with the optic axis parallel to the Z axis, $n = n_{e(o)}$ for the TE (TM) polarization. Furthermore, for the TM polarization, the boundary condition (A 21) indicates that the derivative of the magnetic field along the direction of \mathbf{n}' is continuous, rather than \mathbf{n} . However, in the boundary integral equations (A 13), one involves the derivatives to be with respect to \mathbf{n} . Therefore, in the biaxial crystal, owing to $\varepsilon_a \neq \varepsilon_b$, we cannot easily find the simple transformation between these two direction derivatives. It leads to difficulty in solving the boundary integral equations in the biaxial crystal lens system or in the uniaxial crystal lens system with any orientation of the optic axis, rather than parallel to the Z axis.

References

- [1] See feature issue on *Diffractive Optics Applications, 1995, Appl. Optics*, **34**, 2452.
- [2] HIRAYAMA, K., GLYTSIS, E. N., GAYLORD, T. K., and WILSON, D. W., 1996, *J. opt. Soc. Am. A*, **13**, 2219.
- [3] HIRAYAMA, K., GLYTSIS, E. N., and GAYLORD, T. K., 1997, *J. opt. Soc. Am. A*, **14**, 907.
- [4] PRATHER, D. W., MIROZNIK, M. S., and MAIT, J. N., 1997, *J. opt. Soc. Am. A*, **14**, 34.
- [5] BENDICKSON, J. M., GLYTSIS, E. N., and GAYLORD, T. K., 1998, *J. opt. Soc. Am. A*, **15**, 1822.
- [6] GLYTSIS, E. N., HARRIGAN, M. E., HIRAYAMA, K., and GAYLORD, T. K., 1998, *Appl. Optics*, **37**, 34.
- [7] BLATTNER P., and HERZIG, H. P., 1998, *J. mod. Optics*, **45**, 1395.
- [8] BENDICKSON, J. M., GLYTSIS, E. N., and GAYLORD, T. K., 1999, *J. opt. Soc. Am. A*, **16**, 113.
- [9] HIRAYAMA, K., IGARASHI, K., HAYASHI, Y., GLYTSIS, E. N., and GAYLORD, T. K., 1999, *J. opt. Soc. Am. A*, **16**, 1294.
- [10] YASHIRO K., and OHKAWA, S., 1985, *IEEE Trans. Antennas Propag.*, **AP-33**, 383.
- [11] KAGAMI S., and FUKAI, I., 1984, *IEEE Trans. Microwave Theory Tech.*, **MTT-32**, 455.
- [12] KOSHIBA, M., 1992, *Optical Waveguide Theory by the Finite Element Method* (Tokyo: KTK Scientific), pp. 43–47.
- [13] BASS, M., STRYLAND, E. W. V., WILLIAMS, D. R., and WOLFE, W. L., 1995, *Handbook of Optics, Volume II, Devices, Measurements, and Properties*, 2nd edition (New York: McGraw-Hill), p. 33.66
- [14] BORN, M., and WOLF, E., 1980, *Principles of Optics*, 6th edition (Berlin: Springer-Verlag), pp. 665–667.